Ergodicity of ideal Galerkin three-dimensional magnetohydrodynamics and Hall magnetohydrodynamics models

S. Servidio,[1] W. H. Matthaeus,[1] and V. Carbone[2]
[1]*Bartol Research Institute and Department of Physics and Astronomy, University of Delaware, Newark, Delaware 19716, USA*
[2]*Dipartimento di Fisica, Università della Calabria and Liquid Crystal Laboratory (Licryl/INFM), Ponte P. Bucci Cubo 33B, 87036 Rende (CS), Italy*

(Received 7 June 2008; published 2 October 2008)

We explore the problem of the ergodicity of magnetohydrodynamics and Hall magnetohydrodynamics in three-dimensional, ideal Galerkin systems that are truncated to a finite number of Fourier modes. We show how single Fourier modes follow the Gibbs ensemble prediction, and how the ergodicity of the phase space is restored for long-time Galerkin solutions. Running time averages and two-time correlation functions show, at long times, a convergence towards zero of time averaged single Fourier modes. This suggests a delayed approach to, rather than a breaking of, ergodicity. Finally, we present some preliminary ideas concerning the origin of the associated time scales.

DOI: 10.1103/PhysRevE.78.046302 PACS number(s): 47.52.+j, 52.35.Ra, 52.65.Kj, 47.27.eb

I. INTRODUCTION

Previous studies (see Refs. [1,2], and references therein) have raised interesting questions concerning the robustness of the equilibrium ensemble predictions for finite dimensional representation of ideal, conservative models of fluid and MHD turbulent systems. It has been shown, by using ideal MHD numerical simulations, that, in some particular cases, and for approximately 1000 nonlinear times (or "eddy turnover time," i.e., energy containing length scale/characteristic speed), the time averages of single Fourier modes appear not to follow Gibbs ensemble predictions. This phenomenon has been called "broken ergodicity." The essence of the argument offered to explain this is that the structure of the available phase space is influenced by symmetry properties of the ideal invariants: some of these are scalars (energy) and some are pseudoscalars (helicities). These constraints divide the total phase space into noncommunicating (disconnected) parts; however the equilibrium ensemble assumes ergodicity [1,2], meaning that all parts are accessible to any trajectory. Here we show, by examination of accurate very long time scale numerical simulation, that for two such systems, magnetohydrodynamics (MHD) and Hall magnetohydrodynamics (HMHD), ergodicity is recovered at long times.

It transpires that the earlier reported lack of ergodicity is better described as a perhaps unexpected, and as yet incompletely understood, delay in attaining equivalence of time and ensemble averaging. The origin of the required long time scale for attaining ergodicity is presumably connected to the dynamics of the longest wavelength modes in which a strong condensation of energy is expected for these systems [3–5]. Below we show by graphical evidence, and by direct computation of running time averages and two-time correlation functions that the approach to ergodic behavior is attained in a somewhat unanticipated manner after a delay of thousands of nonlinear times. In particular the evolution of the longest wavelength modes involves random hopping between restricted regions of phase space, a phenomenon closely connected with the appearance of long time tails on the two time autocorrelation functions. Nevertheless, after adequately long times of integration, there is no indication of nonergodic behavior.

The equilibrium Gibbs ensemble model for ideal fluids is not a realistic model for high Reynolds number dissipative turbulence. However, it has been frequently employed [3,6,7] to understand various aspects of the statistical tendencies for spectral transfer in more realistic flows. For example, if a particular quantity tends to accumulate at the largest scales in the Gibbs model, it may signify an inverse cascade in a real dissipative system.

The accuracy of the Gibbs ensemble approach is based upon several factors. The first is an appropriate Liouville theorem [8] in the phase space of real and imaginary parts of the Fourier coefficients [7]. Second there is the assumption that the dynamical solutions obey an ergodic property subject to known constraints. In this, the phase space ensemble averages discussed in the Gibbs theory are taken as equivalent to time averages, for sufficiently large averaging periods [9]. This principle is frequently associated with the assumption that the phase point that describes the system state may be found with equal probability anywhere in the accessible phase space, the sole qualification being that all points on the phase trajectory preserve the numerical values of the ideal invariants that are established by the initial data. If ergodicity appears to be violated given a particular set of known constants of the motion, it may imply that additional constants of motion exist but have been overlooked. If ergodicity appears to be a good approximation, it suggests that additional constants of the motion do not exist, as these might permanently restrict the phase space, causing the failure of Gibbs ensemble predictions. However, even with the correct set of constraints, there is no completely general *a priori* estimate for the time scale required for ergodic behavior to be approximated. However, estimates (known as the classical ergodic theorem) exist for characterizing the approach to ergodicity in a limited sense if the two-time correlations are known to converge rapidly to zero at long times [10].

The equations of incompressible, ideal, constant density three-dimensional (3D) Hall MHD in usual dimensionless units are given by [11]

 ©2008 The American Physical Society

$$\frac{\partial \mathbf{v}}{\partial t} = -(\mathbf{v}\cdot\nabla)\mathbf{v} + (\mathbf{b}\cdot\nabla)\mathbf{b} - \nabla p^*, \tag{1}$$

$$\frac{\partial \mathbf{b}}{\partial t} = (\mathbf{b}\cdot\nabla)\mathbf{v} - (\mathbf{v}\cdot\nabla)\mathbf{b} - \epsilon\nabla \times [(\nabla\times\mathbf{b})\times\mathbf{b}], \tag{2}$$

$$\nabla\cdot\mathbf{v} = 0, \tag{3}$$

$$\nabla\cdot\mathbf{b} = 0. \tag{4}$$

The velocity and magnetic field $\mathbf{v}$ and $\mathbf{b}$ are both written in Alfvén speed units. The magnetic vector potential $\mathbf{a}$ is defined by $\mathbf{b}=\nabla\times\mathbf{a}$ and $\nabla\cdot\mathbf{a}=0$. The total pressure p^* is obtained from the velocity solenoidal equation (3). The parameter ϵ is the ratio between the ion skin depth λ_i and the unit length scale L_0. The time unit is the Alfvén time at L_0. When $\epsilon=0$ the above model reduces to ordinary resistive, viscous incompressible MHD.

By considering a 3D Cartesian box with sides of dimensionless length 2π, and assuming periodicity, the velocity field $\mathbf{v}$ and the magnetic field $\mathbf{b}$ can be written as follows:

$$\mathbf{v}(\mathbf{x},t) = \sum_{\mathbf{k}\in\{\mathbf{N}\}} \mathbf{v}(\mathbf{k},t)\exp(i\mathbf{k}\cdot\mathbf{x}),$$

$$\mathbf{b}(\mathbf{x},t) = \sum_{\mathbf{k}\in\{\mathbf{N}\}} \mathbf{b}(\mathbf{k},t)\exp(i\mathbf{k}\cdot\mathbf{x}), \tag{5}$$

where $\mathbf{N}$ is a set of 3D wave vectors $\mathbf{k}$ such that $k_{\min}\leqslant|\mathbf{k}|\leqslant k_{\max}$. Moreover the reality condition must be satisfied:

$$\mathbf{v}(\mathbf{k},t) = \mathbf{v}^*(-\mathbf{k},t),$$

$$\mathbf{b}(\mathbf{k},t) = \mathbf{b}^*(-\mathbf{k},t). \tag{6}$$

In this paper we will denote as N the number of Fourier modes (vectors) that belong to $\mathbf{N}$. In a Cartesian representation $N=(2N_{\text{box}}+1)^3$. For the cases usually considered, the relevant (or, isolating) ideal invariants are quadratic in the Fourier coefficients of velocity field $\mathbf{v}(\mathbf{k},t)$ and magnetic field $\mathbf{b}(\mathbf{k},t)$ (note that the time argument t will be suppressed below).

For example, for three-dimensional incompressible HMHD in a periodic domain there are three known invariants, all of them quadratic [12,13]. These are the energy per unit mass

$$E = \frac{1}{2V}\int (|\mathbf{v}|^2 + |\mathbf{b}|^2)d^3x \tag{7}$$

$$= \frac{1}{2}\sum_{\mathbf{k}\in\{\mathbf{N}\}} [|\mathbf{v}(\mathbf{k})|^2 + |\mathbf{b}(\mathbf{k})|^2]$$

$$= \sum_{\mathbf{k}\in\{\mathbf{N}\}} [E_v(\mathbf{k}) + E_b(\mathbf{k})], \tag{8}$$

the generalized helicity

$$H_g = \frac{1}{2V}\int \left[\mathbf{v}\cdot\mathbf{b} + \frac{\epsilon}{2}(\boldsymbol{\omega}\cdot\mathbf{v})\right]d^3x \tag{9}$$

$$= \frac{1}{4}\sum_{\mathbf{k}\in\{\mathbf{N}\}} \Big(\mathbf{v}(\mathbf{k})\cdot\mathbf{b}^*(\mathbf{k}) + \mathbf{v}^*(\mathbf{k})\cdot\mathbf{b}(\mathbf{k}) + i\frac{\epsilon}{2}\{[\mathbf{k}\times\mathbf{v}(\mathbf{k})]\cdot\mathbf{v}^*(\mathbf{k}) - [\mathbf{k}\times\mathbf{v}^*(\mathbf{k})]\cdot\mathbf{v}(\mathbf{k})\}\Big), \tag{10}$$

and the magnetic helicity

$$H_m = \frac{1}{2V}\int \mathbf{a}\cdot\mathbf{b}d^3x$$

$$= \frac{1}{4}\sum_{\mathbf{k}\in\{\mathbf{N}\}} \frac{i}{k^2}\{[\mathbf{k}\times\mathbf{b}(\mathbf{k})]\mathbf{b}^*(\mathbf{k}) - [\mathbf{k}\times\mathbf{b}^*(\mathbf{k})]\cdot\mathbf{b}(\mathbf{k})\}. \tag{11}$$

When the Hall parameter $\epsilon\to 0$, the HMHD model reverts to the standard ideal MHD model, and the generalized helicity invariant H_g reduces to the cross helicity $H_c=\frac{1}{2V}\int\mathbf{v}\cdot\mathbf{b}d^3x$.

The crucial point is that when all the invariant quantities are quadratic, the ensemble average for single modes gives for each Cartesian component j [5]:

$$\langle v_j(\mathbf{k})\rangle = \langle b_j(\mathbf{k})\rangle = 0. \tag{12}$$

However, if large parts of the phase space are inaccessible to the trajectory, the time average of every Fourier modes may be nonzero, contradicting Eq. (12). Thus, averaging over the whole phase space, the Gibbs ensemble may not be expected to give an accurate picture of the system. This phenomenon has been called broken ergodicity [1,2]. Here we will comment mainly on the accuracy of Eq. (12); however, we revisit later the structure and number of invariant quantities.

II. GALERKIN APPROXIMATION

By using Eq. (5), the projection of Eqs. (1)–(4) onto a finite set of Fourier wave vectors is given by the following set of equations:

$$\frac{\partial \mathbf{v}(\mathbf{k})}{\partial t} = i\sum_{\mathbf{p}+\mathbf{q}=\mathbf{k}} \{[\mathbf{k}\cdot\mathbf{b}(\mathbf{p})]\mathbf{b}(\mathbf{q}) - [\mathbf{k}\cdot\mathbf{v}(\mathbf{p})]\mathbf{v}(\mathbf{q})\},$$

$$\frac{\partial \mathbf{b}(\mathbf{k})}{\partial t} = \sum_{\mathbf{p}+\mathbf{q}=\mathbf{k}} (i[\mathbf{k}\cdot\mathbf{b}(\mathbf{p})]\mathbf{v}(\mathbf{q}) - i[\mathbf{k}\cdot\mathbf{v}(\mathbf{p})]\mathbf{b}(\mathbf{q}) - \epsilon\{\mathbf{k}\cdot[\mathbf{p}\times\mathbf{b}(\mathbf{p})]\mathbf{b}(\mathbf{q}) + [\mathbf{k}\cdot\mathbf{b}(\mathbf{p})][\mathbf{q}\times\mathbf{b}(\mathbf{q})]\}). \tag{13}$$

The sum is extended on every possible $\mathbf{p}$ and $\mathbf{q}$ that satisfy $\mathbf{p}+\mathbf{q}=\mathbf{k}$, where $\{\mathbf{k},\mathbf{p},\mathbf{q}\}\in\mathbf{N}$, taking care of Eq. (6). Ordinary MHD is recovered when $\epsilon=0$. The time scale of interest is the characteristic nonlinear time (or, in this normalization, the Alfvén time), $\tau=L/U$ for characteristic energy-containing length L, and characteristics speed U. For the numerical results shown below, simulations of Eq. (13) were performed using a Galerkin spectral method code that very accurately

TABLE I. Table of HMHD and MHD runs. In all cases $E=1$. The MHD runs are the ones with $\epsilon=0$ ($H_g \to H_c$). For every case we have chosen $N_{\text{box}}=5$. The column "Δt" lists the time step of the Runge-Kutta technique; "RK" indicates the order of the Runge-Kutta time splitting; the last column indicates the error on global quantities at $t=10\,000$. The error is evaluated as $[F(t)-F(t=0)]/F(t=0)$ (where $F=E,H_g,H_m$), and is reported in percent. Even after many eddy-turnover times, this numerical error, due to the precision of the Galerkin spectral technique, is very small.

Run	H_m	$H_g(H_c)$	ϵ	Δt	RK	error (%)
I	0.17	0.25	1/3	5×10^{-3}	2nd	2.0
II	0.16	5.0×10^{-3}	1/3	5×10^{-3}	2nd	3.0
II	7.0×10^{-6}	0.4	1/3	5×10^{-3}	2nd	0.3
IV	-1.25×10^{-7}	4.1×10^{-6}	1/3	5×10^{-3}	2nd	0.85
V	0.17	0.25	1/3	2×10^{-3}	2nd	0.5
VI	0.16	5.0×10^{-3}	1/3	2×10^{-3}	2nd	0.9
VII	7.0×10^{-6}	0.4	1/3	2×10^{-3}	2nd	0.18
VIII	-1.25×10^{-7}	4.1×10^{-6}	1/3	2×10^{-3}	2nd	0.25
IX	0.16	0.23	0	2×10^{-3}	2nd	0.13
X	0.155	$8.0\times10-3$	0	2×10^{-3}	2nd	0.043
XI	2.0×10^{-7}	0.4	0	2×10^{-3}	2nd	0.035
XII	-1.2×10^{-5}	2.0–6	0	2×10^{-3}	2nd	0.13
XIII	0.16	0.23	0	2×10^{-3}	3rd	0.015

conserves E, H_m, and H_g, apart from round-off and time integration errors. Typically we employ $E=1$ and $L=1$ so the simulation units are in nonlinear time units. For more details on the simulations, see Ref. [5].

Based on comparisons of spectral moments computed from the canonical ensemble, the microcanonical ensemble, and time averages of low truncations of 2D hydrodynamics [9], we might expect that the number of modes retained in our simulations ($N_{\text{box}}=5$) is sufficient to provide agreement with the rugged invariant spectra predicted by the absolute equilibrium.

III. NUMERICAL RESULTS

In order to verify the robustness of Eq. (12), we did several numerical tests, listed in Table I, in which we analyzed the time average of single Fourier modes. First we look at the phase-space trajectory of the real and imaginary part of the field components.

In Fig. 1 this trajectory for several time-snapshots is shown. In this run (run IX) the magnetic helicity and the cross helicity are nonzero. In the initial stage of the time evolution (first panel), the phase-space trajectory seems to be trapped in a quadrant of the space. However, this effect is ephemeral, as it is in all other cases we examined. In every case, the phase space becomes progressively more filled for increasing time, in a way that appears to be consistent with filling the allowed space entirely as $t\to\infty$. This behavior is statistically the same for every component of the field, for both magnetic and velocity field, for both MHD and HMHD, for every set of initial conditions we have examined, for different choices of simulation parameters, and for different numerical techniques. A frequently occurring pattern is the one seen in Fig. 1—the trajectory seems to be trapped in a subspace for some thousands of nonlinear times but, as the time goes on, the phase space is ergodically filled. Thus, one

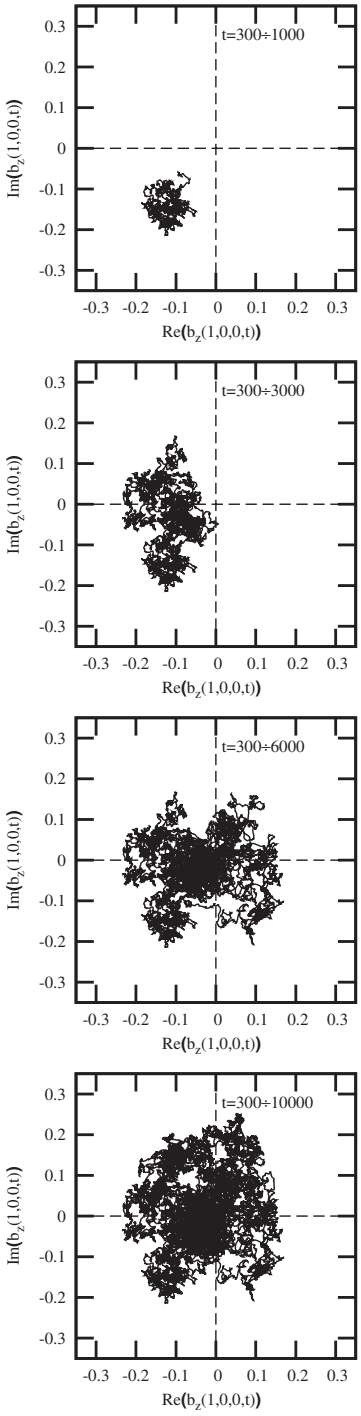

FIG. 1. Time trajectory of a single Fourier mode, imaginary vs real part, for $b_z(1,0,0,t)$ (run IX). All the other components of the magnetic and velocity field have a similar behavior. Initially the trajectory seems to be trapped in a quadrant of the phase space ($t=300-1000$), but when $t\to\infty$ the phase space is ergodically full-filled (lower panel). In other words, the time average of every Fourier mode is consistent with the ensemble prediction of Eq. (12).

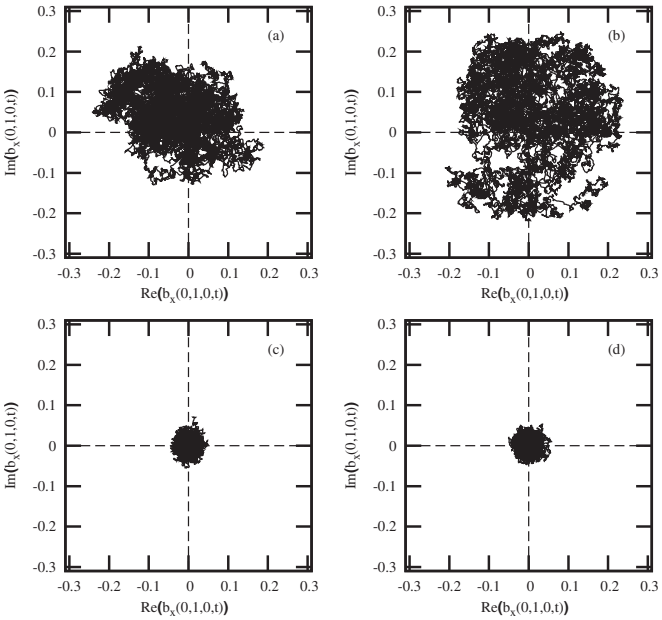

FIG. 2. Time traces of $b_x(0,1,0,t)$ (imaginary vs real part), for several initial conditions: (a) run V, (b) run VI, (c) run VII, and (d) run VIII. See Table I for more details. The ergodic behavior is in good agreement with Eq. (12). Similar results are obtained for all the runs listed in Table I.

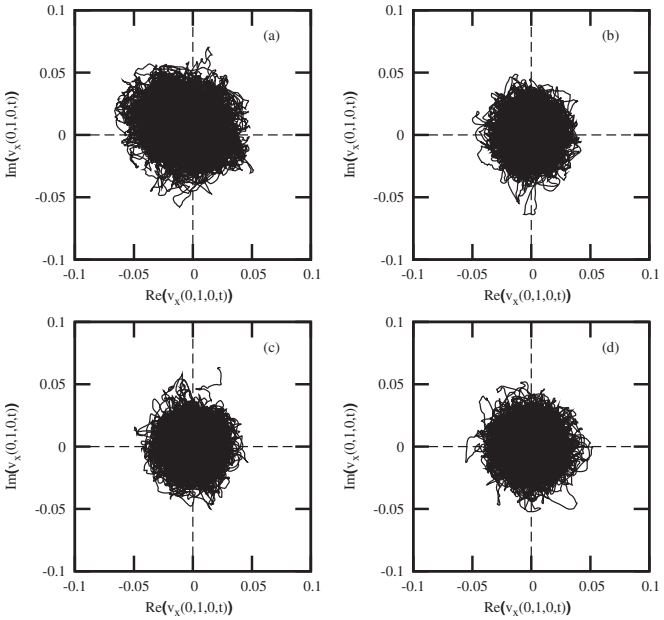

FIG. 3. Time traces of $v_x(0,1,0,t)$ (imaginary vs real part), for the same parameters and initial conditions of Fig. 2. Note that the spreading of these trajectories is much smaller with respect to the magnetic field. This is simply related to the fact that the $\langle E_v(k_{\min})\rangle \ll \langle E_b(k_{\min})\rangle$.

may say that the trajectory temporarily inhabits a restricted portion of phase space, and then, with a time scale of a few hundreds or thousands of time units, hops into another energetically allowed restricted region. The net effect after many hops, is an approach to ergodicity.

We would like to remark that Galerkin simulations are very accurate, free of aliasing errors, and conserve all invariants very accurately. The only error is round-off, and a small controllable time integration error. These are very small. In Table I we report representative errors for each run, defined as the fractional error in the computed energy. As shown in this table, the set of runs we examined included several initial conditions (and different values of helicities). Moreover, we varied the time step of the integration, and the time-integration scheme, going from second to third order Runge-Kutta (RK) technique. In all the cases mentioned above, results described above remain unchanged, and confirm the ergodicity assumed in the Gibbs ensemble.

Figure 2 illustrates the long time behavior of single Fourier components with a lowest allowed wave number (0,1,0) (longest allowed wavelength), for different values of helicities (runs V, VI, VII, and VIII). Although the accessible phase space is more-or-less isotropically covered by the trajectory in each of these cases, there are some interesting differences between runs in which a finite amount of H_m is present and runs with $H_m=0$. When global magnetic helicity is imposed, the trajectory has larger fluctuations around the zero-mean value. This can be explained as follows. The variance (or energy) of large scale modes is higher when $H_m \neq 0$. This is expected in the equilibrium ensemble [5,14] and is related to the condensation of magnetic helicity into the longest allowed wavelength in a modified thermodynamic limit [5,14,15]. In other words, the spreading of the trajectory is proportional to the energy present in that Fourier mode. When $H_m=0$, there is no condensation of helicity into $k_{\min}$, so the variance is smaller at this k vector. This can be seen by comparing Figs. 2(a) and 2(b), with Figs. 2(c) and 2(d).

Another important remark is that less kinetic energy condenses into $k_{\min}$ than magnetic energy. This affects the phase-space trajectories as well—compare Figs. 2 and 3. Specifically, condensation of kinetic energy occurs only if both magnetic helicity and generalized (or cross) helicity are nonzero [5,14]. Inspection of many such trajectory plots (not shown) reveals that higher wave number modes fill their available phase space quickly and approach ergodicity faster. They fluctuate around zero mean within similar circular regions, but with smaller radius, because the amount of available energy is smaller.

IV. TIME AVERAGES AND CORRELATION FUNCTIONS

In order to melt any doubt about the purported nonergodicity of ideal MHD (and Hall MHD too), we computed the time average of single Fourier modes, defined as

$$\langle f_j(\mathbf{k},t,t_0)\rangle_t = \frac{1}{t-t_0}\int_{t_0}^{t} f_j(\mathbf{k},\tau)d\tau, \tag{14}$$

where $f_j=\{v_j,b_j\}$ and $t_0=500$. (The latter value to avoid initial transient effects.) In Fig. 4 the time behavior of Eq. (14), evaluated for several components of both fields, at smallest k, is shown. It takes $t\sim 10\,000$ nonlinear times (or even more) to reach the ensemble asymptotic behavior $\langle f_j\rangle=0$.

This issue is closely related to an interesting work by Kells and Orszag [9]. They performed statistical analysis of

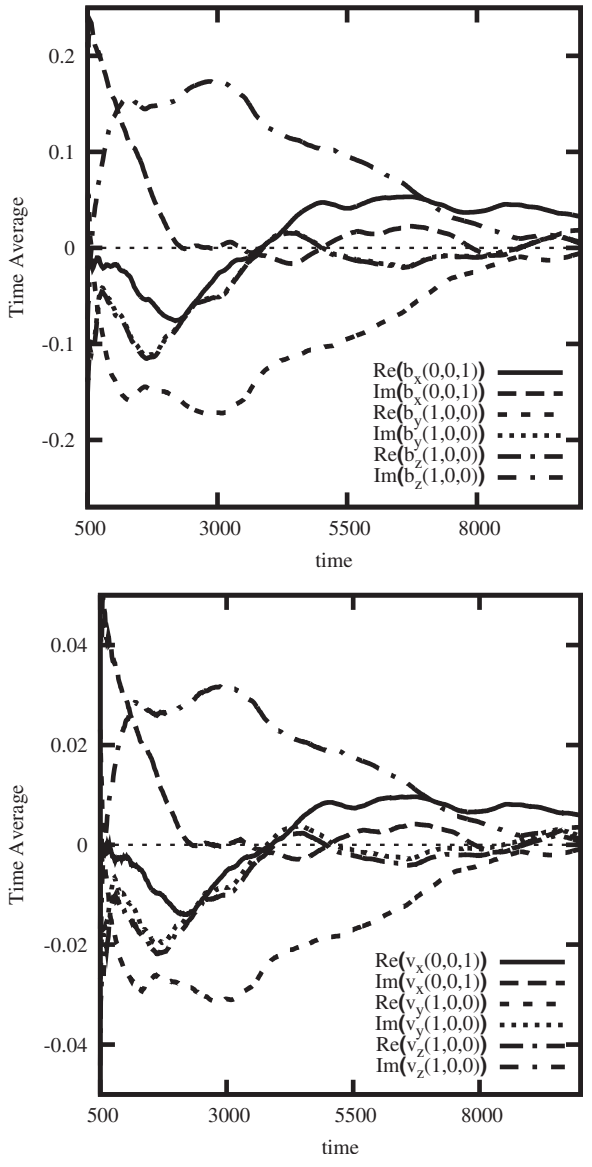

FIG. 4. Running time averages (14), evaluated for a few magnetic (top panel) and velocity (lower panel) field modes (run V). The modes chosen are those that average to zero slowly and therefore are candidates for suggesting broken ergodicity if the averages are truncated after short times. (In Shebalin's work he typically computes averages to about 1000 turnover times.) Here, the time averages tend to zero after 5000 to 8000 turnover times. During these fluctuations toward zero, the velocity and magnetic field modes approximately satisfy Eq. (18) [16,17].

various low-order truncations of two-dimensional inviscid Navier-Stokes, examining the randomness (ergodicity) of the system. They demonstrated numerically the ergodicity of solutions of all isotropically truncated models for which the wave number cutoff is large enough to ensure that every mode is involved in nontrivial interactions. In other word, in systems with many degrees of freedom, there is a strong evidence that the statistical descriptions of the microcanonical ensemble is very accurate for low-order, ideal truncations.

In this pioneering work [9] it was suggested and proved numerically that as the wave number cutoff increases, the probability of any nonrandomness (or nonergodicity) is minimal. This was accomplished by examination of time-averaged energies and time correlations of individual modes. In an analogous way we define the two-time correlation function r of each mode as

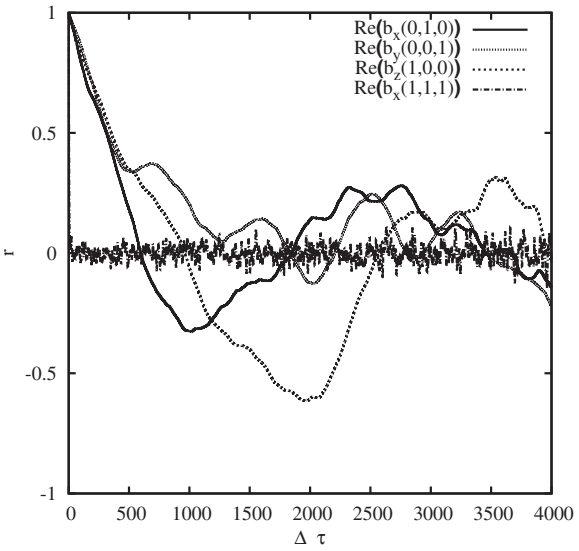

FIG. 5. Time correlations $r(\mathbf{k},T,\Delta t)$, defined by Eq. (15), for several modes (run XIII). In this case $T=6000$. The autocorrelation function indicates that the system is mixing randomly. There is no case in which it saturates to constant value at $t\to\infty$ [9]. The higher k vectors approach zero faster than the smaller ones. The erratic behavior of these modes constitutes evidence that low order truncation of the MHD and HMHD equations are ergodic.

$$r(\mathbf{k},T,\Delta t) = \frac{\int_0^{T-\Delta t}[f_j(\mathbf{k},s)f_j(\mathbf{k},s+\Delta t)ds]}{\sqrt{\left\{\int_0^{T-\Delta t}[f_j(\mathbf{k},s)]^2 ds\right\}\left\{\int_0^{T-\Delta t}[f_j(\mathbf{k},s+\Delta t)]^2 ds\right\}}}. \tag{15}$$

This function r has been normalized so that $r(\mathbf{k},t,0)=1$, and at all times has an absolute value less than or equal to 1. For a mixing (ergodic) system, the values of f_j at large time separations should become statistically independent. If r does not approach 0 but to a constant value as $\Delta t\to\infty$, then the system is not mixing. An erratic approach to 0 (other than a smoothly decaying oscillation) is a consequence of the few degrees of freedom in the truncation. In this way is possible to demonstrate whether the system behaves as if it were ergodic with respect to quantities which are of practical interest.

In Fig. 5 we report the time correlations $r(\mathbf{k},T,\Delta t)$, defined by Eq. (15), for several modes. The autocorrelation function indicates that the system is mixing randomly. In every run listed in Table I we found similar results: there is no case in which $r\to$const as $t\to\infty$. The higher k vectors

approach to zero faster than $k_{\min}$. The erratic behavior of the lowest modes constitutes evidence that low order truncation of MHD and HMHD equation are ergodic. The behavior of r furnishes strong evidence in favor of a statistical description for three-dimensional, truncated, MHD, and HMHD flows, even though for some modes (the lowest k modes), the approach to ergodicity is delayed by what are evidently long correlation time scales. It has been argued that the only cases in which nonergodicity is possible [9,18] are those with a very low number of degrees of freedom, in which cases there are only very limited and trivial nonlinear couplings. Evidently, in the cases treated here, we are very far from this case, even if the number of degrees of freedom (=2662) is not extremely large ($N_{\text{box}}=5$, 11^3 wave vectors, two real solenoidal vector fields).

V. THEORETICAL DISCUSSION AND CONCLUSIONS

We have considered the time behavior the individual Fourier coefficients in ideal MHD and Hall MHD models with a finite number of degrees of freedom. The above results show by example that most of the complex Fourier coefficients approach a zero time average in a time scale of the order of a few nonlinear eddy-turnover times. However, a few coefficients show a delayed evolution towards a zero time average—these are the degree of freedom associated with inverse transfer or condensation into the longest wavelength modes [5,14,15]. The existence of such condensation in MHD and HMHD is connected with nonzero conserved magnetic helicity.

The pattern emerges that these special long wavelength modes randomly hover around nonzero values for times long compared to the eddy turnover time. Eventually, over time scales of hundreds to thousands of nonlinear times, these modes erratically hop to a new pattern, wandering about another nonzero value in a restricted region of the allowed phase space. This continues for at least hundreds or thousands of turnover times, and eventually the sampled regions of phase space cover all regions permitted by the conservation laws. In this time limit ergodicity is fully realized, as far as the numerical experiments can show. This phenomenon, while incompletely understood, is numerically robust. Evidently, during the observed long periods of wandering about nonzero values, the highly energetic long wavelength modes remain in quasiequilibrium with the numerous but much less energetic sea of shorter wavelength Fourier modes. In future research we plan to investigate in detail how this interaction gives rise to the observed long time scales. However, at present we can conclude that we are observing a delayed approach to ergodicity, rather than a breaking of ergodicity.

What would it have implied if we had not observed an approach to zero time averages? The Gibbs ensemble implies a Gaussian distribution, that is, an n-dimensional normal distribution. The joint distribution of l random variables $(x_1, x_2, \ldots, x_l)$ (in our case the imaginary and real parts of velocity and magnetic fields give $l=8$) would then have the form [5,15,19–21]

$$P(x_1,x_2,\ldots,x_l) = \frac{1}{\sqrt{(2\pi)^l \det[\lambda_{jk}]}} \times \exp\left[-\frac{1}{2}\sum_{i=1}^{l}\sum_{j=1}^{l}\Lambda_{ij}(x_i-\psi_i)(x_j-\psi_j)\right], \tag{16}$$

where $(\psi_1, \psi_2, \ldots, \psi_l)$ are the mean values, and $[\lambda_{ij}]=[\Lambda_{ij}]$ is the moment matrix [19–21]. If Eq. (12) is not satisfied, the mean values enter Eq. (16) through nonzero values of $\{\psi_j\}$. In particular,

$$\langle (x_i-\psi_i)(x_k-\psi_k)\rangle = \lambda_{ik}. \tag{17}$$

If $\psi_j \neq 0$ then every ensemble prediction that is made under the assumption that $\psi_j=0$ would be wrong. In that case the system would admit another invariant quantity, i.e., the nonzero value of ψ_j that had been overlooked. This would presumably have a physical meaning. However, for the cases of HMHD and MHD we have examined [5] the agreement of the numerical results with the $\psi=0$ case support the view that these additional invariants are not present.

For every simulation listed in Table I we found that the relative error between time averaged spectra and the ensemble predictions is very small, especially after thousands of nonlinear times. This suggests that for $t\to\infty$ the time average of any quantity (in MHD and HMHD both) coincide exactly with the equilibrium obtained by the Gibbs ensemble method.

Note that the ensemble spectral predictions become reasonably accurate estimates of the long wavelength spectra even at times prior to attaining full ergodicity. This is naturally explained by noting that the points about which the temporary wanderings occur are evidently equivalent to one another. This seems to reflect the low order degeneracy of the longest wavelength modes, and provides an important clue to guide efforts to explain the long time scale phase space wandering.

Another interesting phenomenon, as can be inferred from Fig. 4, is that the large scale modes that converge slowly to zero average do so while obeying some particular relations. In the HMHD case, these fluctuations are near to the minimum energy solutions known as double Beltrami flows [16,17,22–24]. These special states are obtained from a variational principle, and are given by

$$\mathbf{v}(\mathbf{k}) = \alpha_1 \mathbf{b}(\mathbf{k}) + i\alpha_1 \epsilon \mathbf{k}\times\mathbf{v}(\mathbf{k})$$

$$\mathbf{b}(\mathbf{k}) = i\frac{(1-\alpha_1^2)}{\alpha_2}\mathbf{k}\times\mathbf{b}(\mathbf{k}) + \frac{\alpha_1^2}{\alpha_2}\epsilon\mathbf{k}\times[\mathbf{k}\times\mathbf{v}(\mathbf{k})]. \tag{18}$$

The constants α_1 and α_2 are functions of the Lagrange multipliers. In the MHD case ($\epsilon=0$) the previous equations

reduce to the well-known force free and Alfvénic states [24]. It is important to notice that this kind of temporary fluctuations cannot be described in the Gibbs ensemble framework, and so this topic goes beyond the purpose of this paper. We plan to revisit several of these extended issues in a future publication.

ACKNOWLEDGMENTS

This research was supported in part by NSF Grant No. ATM-0539995 and NASA Grants No. NNX07AR48G, No. NNX08AI47G (Heliophysics Theory), and No. NNX08AT76G (MMS Theory Support).

[1] J. V. Shebalin, Physica D **37**, 173 (1989).
[2] J. V. Shebalin, Phys. Lett. A **250**, 319 (1998).
[3] R. H. Kraichnan, Phys. Fluids **10**, 1457 (1967).
[4] R. H. Kraichnan and S. Chen, Physica D **37**, 160 (1989).
[5] S. Servidio, W. H. Matthaeus, and V. Carbone, Phys. Plasmas **15**, 042314 (2008).
[6] R. H. Kraichnan and D. Montgomery, Rep. Prog. Phys. **43**, 547 (1980).
[7] D. Fyfe and D. Montgomery, J. Plasma Phys. **16**, 181 (1976).
[8] T. D. Lee, Q. Appl. Math. **10**, 69 (1952).
[9] L. C. Kells and S. A. Orszag, Phys. Fluids **21**, 162 (1978).
[10] V. S. Pugachev, *Theory of Random Functions and its Application to Problems of Automatic Control* (State Press for Technical and Theoretical Literature, Moscow, 1957).
[11] T. J. M. Boyd and J. J. Sanderson, *The Physics of Plasmas* (Cambridge University Press, Cambridge, 2003).
[12] L. Turner, IEEE Trans. Plasma Sci. **PS-14**, 849 (1986).
[13] S. Ohsaki and Z. Yoshida, Phys. Plasmas **12**, 064505 (2005).
[14] T. Stribling and W. H. Matthaeus, Phys. Fluids B **2**, 1979 (1990).
[15] U. Frisch, A. Pouquet, J. Léorat, and A. Mazure, J. Fluid Mech. **68**, 769 (1975).
[16] P. D. Mininni, D. O. Gómez, and S. M. Mahajan, Astrophys. J. **567**, L81 (2002).
[17] S. Ohsaki and Z. Yoshida, Phys. Plasmas **12**, 064505 (2005).
[18] O. H. Hald, Phys. Fluids **19**, 914 (1976).
[19] L. D. Landau and E. M. Lifshitz, *Statistical Physics*, Volume 5 of Course of Theoretical Physics (Addison-Wesley, New York, 1959), pp. 343–353.
[20] G. A. Korn and T. M. Korn, *Mathematical Handbook for Scientists and Engineers* (Dover, Mineola, NY, 2000), pp. 609–636.
[21] S. Servidio and V. Carbone, Phys. Rev. Lett. **95**, 045001 (2005).
[22] J. V. Shebalin, Phys. Plasmas **1**, 541 (1994).
[23] J. V. Shebalin, Phys. Plasmas **14**, 102301 (2007).
[24] S. Servidio, W. H. Matthaeus, and P. Dmitruk, Phys. Rev. Lett. **100**, 095005 (2008).